THE CRITICAL SPEEDS OF A MACHINE TOOL SPINDLE-BEARING SYSTEM WITH THE HIGH STIFFNESS HYDROSTATIC JOURNAL BEARINGS

Y. S. Chen, Y. D. Cheng, and C. C. Chiou
Department of Mechanical Engineering
Yuan-Ze University
Chungli, Taoyuan, Taiwan

INTRODUCTION

The ordinary hydrodynamic bearings have been replaced by the hydrostatic bearings in the application of machine tools in recent years. For the hydrodynamic bearings, the journal and the bearing surface are separated by the sliding action with a wedge pressure-generating mechanism to develop a pressure within the bearing. It has advantages of simple structure and cheap cost. However, the fluid film lubrication may break down if the system is at the low rotating speed, or during the startup and shutdown processes.

On the contrary, for the hydrostatic bearings, the journal and bearing surface are separated by a fluid film maintained by a pressure source outside the bearing. The hydrostatic bearings avoid the disadvantages of the hydrodynamic bearings so that they have characteristics of high revolution and high precision, high load capacity, uniform thermal expansion, good working life and predictable performances. With proper design, the bearing stiffness of the hydrostatic bearings even surpasses the typical roller bearings [1]. As a result, the introduction of the hydrostatic bearings in the machine tool can significantly improve the surface finish and quality of the workpiece especially under the high machining speeds and feeds.

One of the key concerns to ensure the reliability of the machinery is to control the distribution of the critical speeds of the spindle system. The regenerative chatter problem that always appears near one of the critical speeds of the system is normally seen during the machining processes. Consequently, the distribution of the critical speeds is a very critical factor that dominates the dynamic properties of the system. With the goal to provide the best performance of the machine tool, this investigation is then intended to predict the critical speeds of the system with the spindle equipped with the high stiffness hydrostatic journal bearings. Those parameters such as the radial clearance, supply pressure, feeding parameter and ratio of bearing length/diameter will be adopted for examining their effects on the bearing stiffness. A realistic spindle model is represented by a number of divided beam elements at the beginning of the study when solving the problem with the self-written finite element method (FEM) program. Later, the modal testing is performed to verify the correctness of the model. Finally, with the verified FEM model, all the trends of the critical speeds of the system are explored by varying the number of feeding rows in the hydrostatic bearings.

CRITICAL SPEEDS ESTIMATION

As addressed above, the FEM model is utilized to represent a real machine tool spindle-bearing system. A Timoshenko beam element involving the shear and rotary inertia effects is formulated in the model as referred to the theoretical background in [2, 3]. Each of the nodes on the element has four degrees of freedom, i.e., the translation and rotation both in the horizontal and vertical directions. By ignoring the external force, the equation of motion of the system can be shown as:

$$[M]\{\ddot{q}\}+[G]\{\dot{q}\}+[K]\{q\}=\{0\} \qquad (1)$$

To solve the critical speeds of system, the eigen-value matrix can be established by substituting $\{q\}=\{h_0\}e^{\alpha t}$ into the system equation:

$$\begin{bmatrix} [0] & [I] \\ -[K]^{-1}[M] & -[K]^{-1}[G] \end{bmatrix} \begin{Bmatrix} \alpha\{h_0\} \\ \{h_0\} \end{Bmatrix} = \frac{1}{\alpha} \begin{Bmatrix} \alpha\{h_0\} \\ \{h_0\} \end{Bmatrix} \qquad (2)$$

Here, the bearing damping coefficients are ignored, hence, the so-called undamped critical speeds are then obtained from the above equation.

MULTI-ARRAY FEEDING BEARINGS

The schematic of the typical 3-row multi-array feeding hydrostatic journal bearings are shown at left in Fig. 1. As illustrated in the figure at right, there are 1-row, 2-row and 3-row of feeding holes design on the spindle. Under the conditions of thin, incompressible lubricant film and lower journal eccentricity ratios, the Reynolds equation can be simplified as [4]:

$$\frac{\partial^2 P}{\partial y^2}+\frac{\partial^2 P}{\partial z^2}=0 \tag{3}$$

The method of separating variables is then introduced here to solve the motion equation. The boundary conditions both at the feeding holes and the bearing sides are set following [5]. The dimensionless load capacity for the 1-, 2- and 3-row feeding journal bearing can be obtained as shown below respectively:

$$\begin{aligned} W_1 &= W_1(\varepsilon, P_s, \lambda, L/D) \\ W_2 &= W_2(\varepsilon, P_s, 4\lambda/3, 2L/3D) \\ W_3 &= W_3(\varepsilon, P_s, \lambda/2, \lambda(3+\lambda)/2(2+\lambda), L/D, L/2D) \end{aligned} \tag{4}$$

where $\varepsilon=e/C$, is the journal eccentricity ratio which is defined as the ratio of the journal eccentricity (e) to the radial clearance of the bearing (C). $P_s=ps/pa$, is the ratio of the supply pressure designated as "*ps*" to the ambient pressure "*pa*", L is the bearing length and D is the bearing diameter. The feeding parameter λ is defined as:

$$\lambda=\frac{3a^4N}{8C^3l_t}\left(\frac{L}{D}\right) \tag{5}$$

where N is the number of feeding tubes in each of the feeding row, a is the radius of the feeding tube and l_t is length of the feeding tube. Besides, throughout the study, the dimensionless bearing stiffness K is defined as the variations of the dimensionless load capacity W to the journal eccentricity ratio ε. It can be shown as:

$$K=\frac{dW}{d\varepsilon} \tag{6}$$

MODAL TESTING OF THE SPINDLE

The configuration of the machine tool spindle for this study is shown in Fig. 2. The spindle is designed with the multi-array feeding hydrostatic journal bearings for satisfying the demands of the high speed and high precision machining processes. It is also shown in the figure that there is a total of 33 elements in the FEM model of the spindle. In reality, the spindle has a total length of 151.3 mm and its outside diameter is 25.25 mm. The rear and front bearings are connected to the spindle with the isotropic bearing stiffness designated as K_b both at node 8 and node 26 respectively.

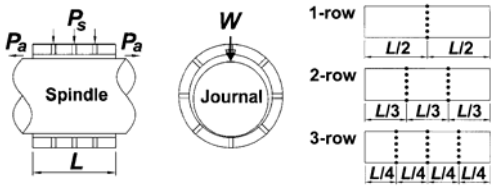

FIGURE 1. The multi-array feeding hydrostatic journal bearing.

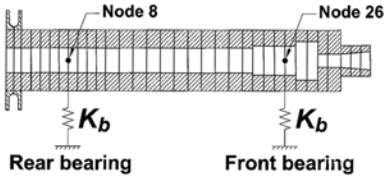

FIGURE 2. Schematic of the finite element model of the spindle-bearing system.

For the correctness verification of the spindle model, an experimental modal testing is conducted right after. During the test, the spindle is suspended with the rubber bands at both ends to simulate the free-free boundary conditions. The results of the FEM model show that the frequencies of the first and second bending modes are at 5,310 Hz and 12,670 Hz respectively. The corresponding modal testing results are at 5,356 Hz and 12,993 Hz respectively. The error percentages of those frequencies based on the experimental results are -0.86% and -2.49% respectively. This indicate that the accuracy of the data resulted from the FEM model is acceptable since all the error percentages are within ±5%.

BEARING STIFFNESS WITH DIFFERENT DESIGN PARAMETERS

In this study, a pair of hydrostatic bearings each with multi-array feeding is built to support the spindle that can provide the system stiffness during the machining process. In the parametric analyses for the effects of various designs on the spindle stiffness, some of the typical values as listed below are chosen for each of the

following bearing parameters. Such as the radial clearance of *C*=15 μm, bearing diameter *D*=25.6 mm, supply pressure *ps*=3.5 MPa, feeding parameter λ =0.73 (i.e., for the case of eight feeding tubes in one feeding row, *N*=8) and the number of feeding rows are all considered initially in the analysis. Among them, one is varied while the others are kept intact with the above mentioned values during each of the analysis process. Some of the effects on the bearing stiffness of these combined parameter variations are illustrated in Fig. 3-Fig. 5 respectively.

Fig. 3 shows the bearing stiffness versus the bearing load and the bearing radial clearance. As indicated in Fig. 3(a), it is obvious that the bearing stiffness is independent of the low bearing load under 2 kg no matter for 1-, 2- or 3-row feeding designs. In other words, this condition is equivalent to the situation of lower journal eccentricity ratios. In Fig. 3(b), the stiffness decreases dramatically with the increase of the bearing radial clearance. For the larger radial clearance of 20-30 μm, the stiffness variations tend to smooth down gradually. As a result, the radial clearance should be designed as small as possible to obtain the largest stiffness.

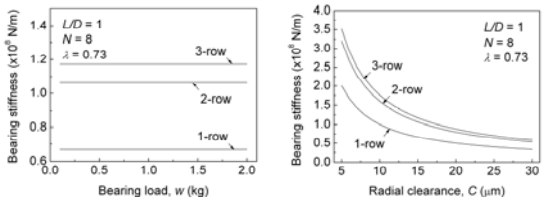

FIGURE 3. Bearing stiffness versus (a) bearing load, and (b) radial clearance.

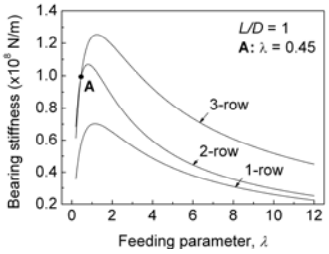

FIGURE 4. Bearing stiffness versus feeding parameter.

The effects of the feeding parameter (i.e. λ) to the bearing stiffness are shown in Fig. 4. There exists an optimum feeding parameter to maximize the bearing stiffness. From the peaks of the curves in the figure, it can be seen the feeding parameters should be limited between λ=0.5-1.5 to obtain the optimum stiffness. However, if λ <0.45 (point A), the stiffness between the 2- and 3-row feeding are fairly identical.

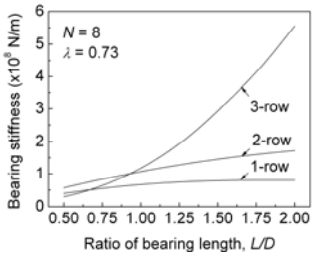

FIGURE 5. Bearing stiffness versus the length/diameter (L/D) ratio of the bearing.

The variation of the bearing stiffness versus the length/diameter (*L/D*) ratio of bearing is shown in Fig. 5. As can be seen in the figure, the bearing stiffness is highly sensitive to the *L/D* ratio for the 3-row feeding bearings but is quite insensitive to the 1- and 2-row feeding bearings. For the case of *L/D*<1, the 2-row feeding bearing is recommended as the best choice to retain the sufficient stiffness. Conversely, the excellent stiffness is resulted for *L/D*>1 with the design of the 3-row feeding bearing.

VARIATIONS OF SYSTEM CRITICAL SPEEDS

The stiffness as resulted from the bearing is introduced to the system when proceeds to the critical speeds analysis. Fig. 6 shows the variations of the critical speeds with the multi-array feeding design at the front and rear bearings correspondingly. As can be seen in the Fig. 6(a), the first critical speeds Ω_1 are insensitive to the front or rear bearing when the 1-row feeding is adopted. However, the first critical speeds are raised obviously if the 2- or 3-row feeding is considered at both bearings. Fig. 6(b) shows the variations of the second critical speeds Ω_2 of the system. It indicates that the second critical speed has increased so rapidly when the rear bearing is switched from 1-row to 2- or 3-row feedings while the front bearing has just 1-row feeding. On the other hand, when the front bearing has 2- or 3-row feeding, the second critical speeds won't have too much change no matter with 1-, 2-, or 3-row feeding in the rear bearing.

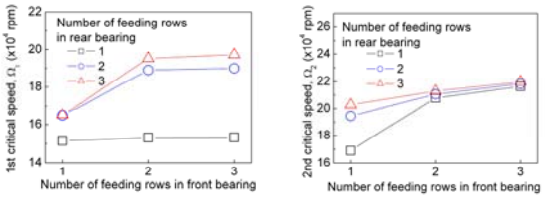

(a) (b)

FIGURE 6. (a) The first critical speed, and (b) the second critical speed of spindle-bearing system.

Fig.7 shows the percentage differences between the first and the second critical speeds of the system. These differences actually reflect the fact about how close or apart the first and second critical speeds are located in the spectrum of the frequency domain. As shown in the figure, when the 1-row feeding is designed on the rear bearing, the differences between the first and second critical speeds are all increased regardless 1-, 2-, or 3-rwo feeding on the front bearing. Similar differences will be observed vice versa. In the mean time, the difference will be reduced for all the cases when both the front and rear bearings has more than 1-row feeding. Finally, it is also noted in the figure that the smallest percentage difference of 9.1% is achieved with the 3-row feeding in the rear bearing and the 2-row feeding in the front bearing.

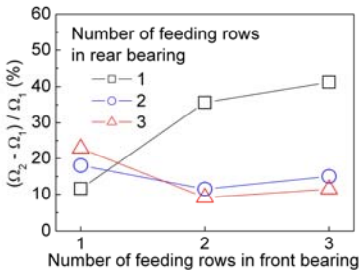

FIGURE 7. The percentage differences between the first and second critical speeds.

CONCLUSIONS

This study has investigated the stiffness characteristics of the multi-array feeding journal bearing with various bearing design parameters. The essential results for the distribution of the system critical speeds have been demonstrated visually to define the proper working speed. All the meaningful results obtained can be summarized as follows:

The bearing stiffness is independent of the bearing load for the low journal eccentricity ratios (i.e. at low bearing load). The stiffness decreases dramatically only if the radial clearance is increased.

There exists the optimum feeding parameters to make the bearing stiffness the highest. To obtain the optimum bearing stiffness, the feeding parameters should be limited to be in the range of λ=0.5-1.5.

The bearing stiffness is the most sensitive to the bearing length/diameter ratio for the 3-row feeding bearing but is insensitive to the 1- and 2-row feeding bearings.

In terms of the variations of the critical speeds, the first critical speeds are insensitive to the front or rear bearing when the 1-row feeding is adopted in either one of the front or rear bearings. The second critical speed increases rapidly by 2- or 3-row feeding either in the rear or front bearings.

The differences between the second and first critical increases steadily when only 1-row feeding is adopted in either the front or rear bearings. The minimum percentage differences can be achieved with the 3-row feeding in the rear bearing and the 2-row feeding in the front bearing.

REFERENCES

[1] Weck M, Koch A. Spindle-Bearings Systems for High-Speed Applications in Machine Tools. Annals of the CIRP. 1993; 42: 445-448.

[2] Nelson HD. A Finite Rotating Shaft Element Using Timoshenko Beam Theory. Journal of Mechanical Design. 1980; 102: 793-803.

[3] Edney SL, Fox CHJ, Williams EJ. Tapered Timoshenko Finite Elements for Rotor Dynamics Analysis. Journal of Sound and Vibration. 1990; 137: 463-481.

[4] Pinkus O, Sternlicht B. Theory of Hydrodynamic Lubrication. McGraw-Hill. New York: 1961.

[5] Su JCT, Lie KN. Approximate Solutions for Hydrostatic Journal Bearings with Multi-Array of Hole-Entry. Lubrication Engineering. 2002; 58: 19-28.